

## CENTIMETER POLARIMETRY OF THE R CORONAE AUSTRALIS REGION

MINHO CHOI<sup>1</sup>, KEN'ICHI TATEMATSU<sup>2</sup>, KENJI HAMAGUCHI<sup>3,4</sup>, AND JEONG-EUN LEE<sup>5</sup>

## ABSTRACT

Circularly polarized 3.5 cm continuum emission was detected toward three radio sources in the R CrA region using the Very Large Array. The Class I protostar IRS 5b persistently showed polarized radio emission with a constant helicity over 8 yr, which suggests that its magnetosphere has a stable configuration. There is a good correlation between the Stokes  $I$  and Stokes  $V$  fluxes, and the fractional polarization is about 0.17. During active phases the fractional polarization is a weakly decreasing function of Stokes  $I$  flux, which suggests that IRS 5b is phenomenologically similar to other types of flare stars such as RS CVn binaries. The variability timescale of the polarized flux is about a month, and the magnetosphere of IRS 5b must be very large in size. The Class I protostar IRS 7A was detected once in circularly polarized radio emission, even though IRS 7A drives a thermal radio jet. This detection implies that the radio emission from the magnetosphere of a young protostar can escape the absorption by the partially ionized wind at least once in a while. The properties of IRS 7A and IRS 5b suggests that Class I protostars have organized peristellar magnetic fields of a few kilogauss and that the detectability of magnetospheric emission may depend on the evolutionary status of protostar. Also reported is the detection of circularly polarized radio emission toward the variable radio source B5.

*Subject headings:* ISM: individual (R Coronae Australis IRS 5) — ISM: structure — stars: flare — stars: formation

## 1. INTRODUCTION

Magnetic fields play an important role in star formation (André 1996; Feigelson et al. 2007; Bouvier et al. 2007). This is especially true in the protostellar accretion/evolution processes, and peristellar magnetic fields are expected or even required in many theoretical models: Protostellar outflows are generated through magnetocentrifugal ejection mechanism (e.g., Pudritz et al. 2007). The magnetorotational instability may provide the viscosity required to explain the dynamics of accretion disks (Balbus & Hawley 1991). Magnetospheres may force the protostellar spin to be coupled with the rotation of circumstellar disk, and the inner edge of accretion disks may be truncated by the magnetosphere near the corotation radius (Camenzind 1990; Königl 1991). The transfer of material from the accretion disk to the protostar may be done through magnetospheric accretion (Bouvier et al. 2007). Despite all these expectations, observational evidence of peristellar magnetic fields of protostars is very difficult to come by.

Much of our knowledge about the peristellar magnetic fields of young stellar objects comes from the observations of T Tauri stars, especially radio continuum observations at centimeter wavelengths (André et al. 1992; André 1996). The key characteristics are the variability and circular polarization of emission from nonthermal electrons. The variability timescale is usually hours to days, much longer than solar-type flares, which implies that large-scale magnetic fields are involved. Moderate degrees of circular polarization were observed, suggesting that the emission mechanism is gyrosynchrotron radiation from mildly

relativistic electrons. The detection of circular polarization at  $\sim 5$  GHz implies a dipole-like large-scale magnetosphere with a surface field strength of  $\sim 1$  kG (Güdel 2002).

X-ray surveys of pre-main-sequence stars suggest that the level of activity decays with stellar age (Preibisch & Feigelson 2005), and we expect that Class I protostars may be magnetically more active than T Tauri stars. However, the free-free absorption by thermal wind is supposed to obscure the magnetosphere of protostars in most cases (André et al. 1992; André 1996). The youngest object detected in circularly polarized radio emission is IRS 5 in the R CrA region (Feigelson et al. 1998). In fact, IRS 5 is the only known protostellar object persistently displaying circularly polarized emission (Forbrich et al. 2006; Miettinen et al. 2008). Therefore, IRS 5 provides a wonderful opportunity to study the magnetic activity of protostars.

To obtain high-quality images of the R CrA region, we observed in the centimeter continuum with the Very Large Array (VLA) of the National Radio Astronomy Observatory. The main results were presented in Paper I (Choi et al. 2008). In this paper, we present the polarimetry of the R CrA region. We describe the data in § 2. In § 3 we briefly report the results of the polarimetry. In § 4 we discuss the star forming activity of the radio sources showing circularly polarized centimeter continuum emission. A summary is given in § 5.

## 2. DATA

We analyzed 14 data sets to measure the circularly polarized flux densities of the centimeter continuum sources in the R CrA region. Details of the observations are described in Paper I. See Table 1 of Paper I for the parameters of the VLA observing runs and the observing track numbers. (The track numbers are preceded by ‘Tr’ throughout this paper.) Maps of circularly polarized (Stokes  $V$ ) intensity were made using a CLEAN algorithm. All the images presented in this paper are corrected for the primary beam response, and the lowest contour level roughly corresponds to the  $3\sigma$  value, where  $\sigma$  is the rms of noise.

The accuracy of polarization calibration of VLA data is usually better than 0.5% for compact sources. For circular polarization measurements, the beam squint can induce spurious signals, which may affect sources located far away from the point-

<sup>1</sup>International Center for Astrophysics, Korea Astronomy and Space Science Institute, Hwaam 61-1, Yuseong, Daejeon 305-348, South Korea; minho@kasi.re.kr.

<sup>2</sup>National Astronomical Observatory of Japan, 2-21-1 Osawa, Mitaka, Tokyo 181-8588, Japan.

<sup>3</sup>Center for Research and Exploration in Space Science and Technology and X-ray Astrophysics Laboratory, NASA Goddard Space Flight Center, Greenbelt, MD 20771.

<sup>4</sup>Department of Physics, University of Maryland, Baltimore County, 1000 Hilltop Circle, Baltimore, MD 21250.

<sup>5</sup>Department of Astronomy and Space Science, Astrophysical Research Center for the Structure and Evolution of the Cosmos, Sejong University, Gunja 98, Gwangjin, Seoul 143-747, South Korea.

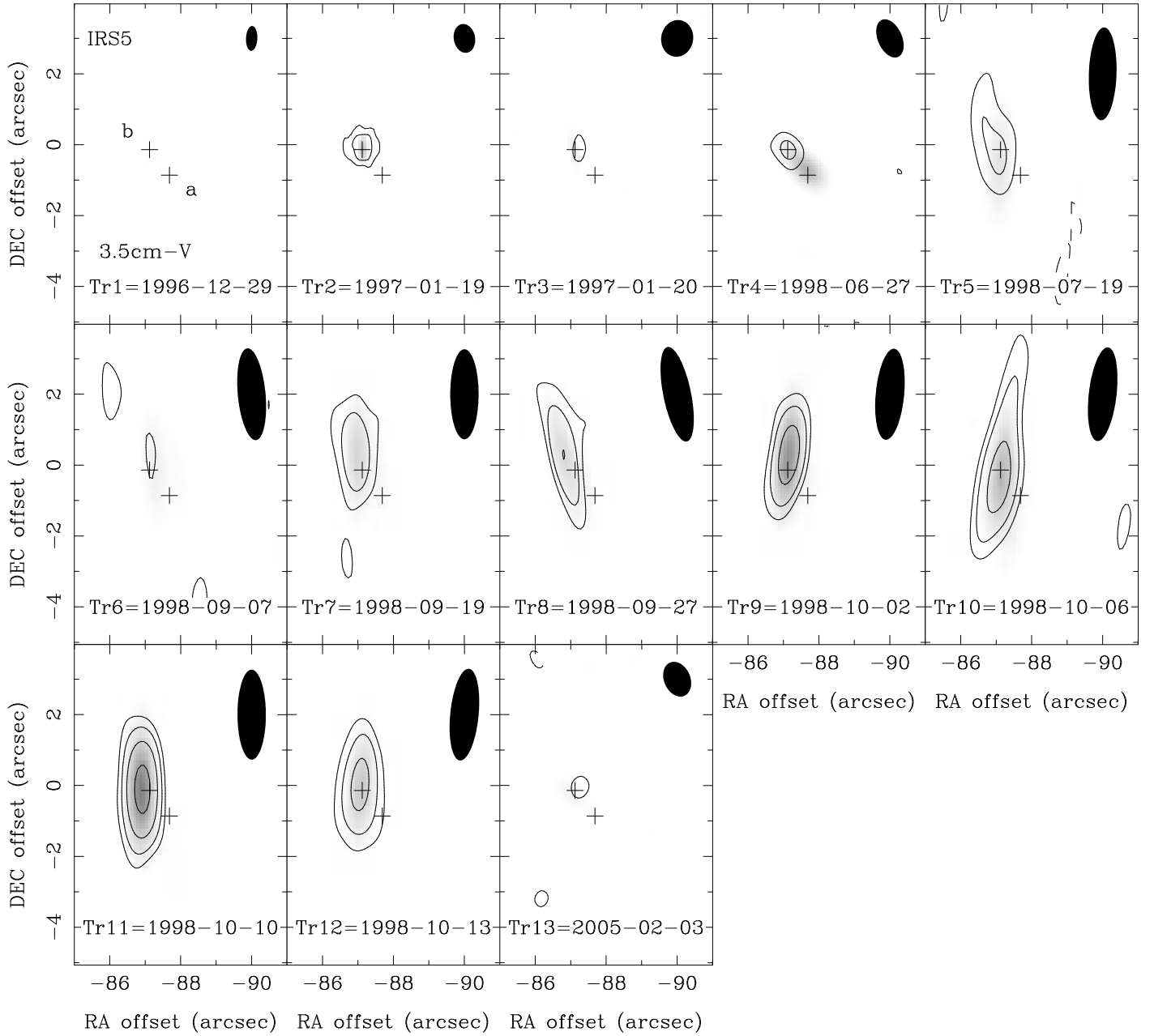


Fig. 1.— Stokes  $V$  natural-weight maps (*contours*) of the 3.5 cm continuum toward IRS 5a/b. Observation dates and track numbers are labeled. A position correction was applied to the Tr 2 and 3 maps (see § 3.2 of Paper I). The contour levels are 1, 2, 4, and 8 times  $0.06 \text{ mJy beam}^{-1}$ . Shown in the top right corner are the synthesized beams (see Table 1 of Paper I). *Gray scale*: Stokes  $I$  maps as shown in Fig. 12 of Paper I. *Plus signs*: Peak positions of the 3.5 cm sources in the uniform-weight Stokes  $I$  map of Tr 1.

ing center. For snapshot images, this effect can be as large as 20% at the edge of the field of view. For the maps made from the data of a whole track, the circular polarization may be accurate to a few percent. This issue will be discussed again at the end of § 3.

### 3. RESULTS

Stokes  $V$  flux was detected toward three sources in the 3.5 cm maps while none of the radio sources showed detectable Stokes  $V$  flux in the 6.2 cm maps. The polarized emission of IRS 5 was reported previously (Feigelson et al. 1998; Forbrich

et al. 2006; Miettinen et al. 2008), and we can now identify the source as IRS 5b. Detections of polarized emission from IRS 7A and B5 are reported here for the first time.

IRS 5b showed detectable polarization in most observing runs, but IRS 5a was never detected in the Stokes  $V$  flux maps (Figs. 1 and 2). The Stokes  $V$  flux densities from the archival data sets are usually, but not always, consistent with the values reported by Feigelson et al. (1998) and Forbrich et al. (2006). Table 1 lists the total flux densities, both Stokes  $I$  and Stokes  $V$  fluxes (hereafter  $I$  and  $V$  fluxes, respectively), and the fractional circular polarization,  $\Pi_c = |V|/I$ , of IRS 5b.

The  $V$  flux from IRS 7A was detected during the obser-

TABLE 1  
FLUX DENSITIES OF IRS 5B AT 3.5 CM

| Track       | Date        | $I$<br>(mJy)    | $V$<br>(mJy)    | $\Pi_c^a$         |
|-------------|-------------|-----------------|-----------------|-------------------|
| Tr 1 .....  | 1996 Dec 29 | $0.25 \pm 0.02$ | ...             | $< 0.24^b$        |
| Tr 2 .....  | 1997 Jan 19 | $1.82 \pm 0.04$ | $0.23 \pm 0.02$ | $0.126 \pm 0.011$ |
| Tr 3 .....  | 1997 Jan 20 | $0.58 \pm 0.04$ | $0.09 \pm 0.02$ | $0.16 \pm 0.04$   |
| Tr 4 .....  | 1998 Jun 27 | $0.53 \pm 0.04$ | $0.15 \pm 0.02$ | $0.28 \pm 0.04$   |
| Tr 5 .....  | 1998 Jul 19 | $0.75 \pm 0.04$ | $0.16 \pm 0.03$ | $0.21 \pm 0.04$   |
| Tr 6 .....  | 1998 Sep 07 | $0.45 \pm 0.04$ | $0.07 \pm 0.03$ | $0.16 \pm 0.07$   |
| Tr 7 .....  | 1998 Sep 19 | $1.05 \pm 0.04$ | $0.22 \pm 0.02$ | $0.21 \pm 0.02$   |
| Tr 8 .....  | 1998 Sep 27 | $0.91 \pm 0.03$ | $0.24 \pm 0.02$ | $0.26 \pm 0.02$   |
| Tr 9 .....  | 1998 Oct 02 | $2.67 \pm 0.04$ | $0.34 \pm 0.02$ | $0.127 \pm 0.008$ |
| Tr 10 ..... | 1998 Oct 06 | $1.83 \pm 0.04$ | $0.42 \pm 0.04$ | $0.23 \pm 0.02$   |
| Tr 11 ..... | 1998 Oct 10 | $3.14 \pm 0.05$ | $0.60 \pm 0.02$ | $0.191 \pm 0.007$ |
| Tr 12 ..... | 1998 Oct 13 | $1.43 \pm 0.04$ | $0.31 \pm 0.02$ | $0.217 \pm 0.015$ |
| Tr 13 ..... | 2005 Feb 03 | $0.41 \pm 0.03$ | $0.08 \pm 0.02$ | $0.20 \pm 0.05$   |

NOTES.—Flux densities are corrected for the primary beam response. The Stokes  $I$  fluxes are the same as given in Table 5 of Paper I. The Stokes  $V$  fluxes are from the natural-weight maps.

<sup>a</sup> Fractional circular polarization.

<sup>b</sup> Stokes  $V$  flux was undetected in Tr 1. The upper limit of  $\Pi_c$  was calculated with the  $3\sigma$  value of the  $V$  map.

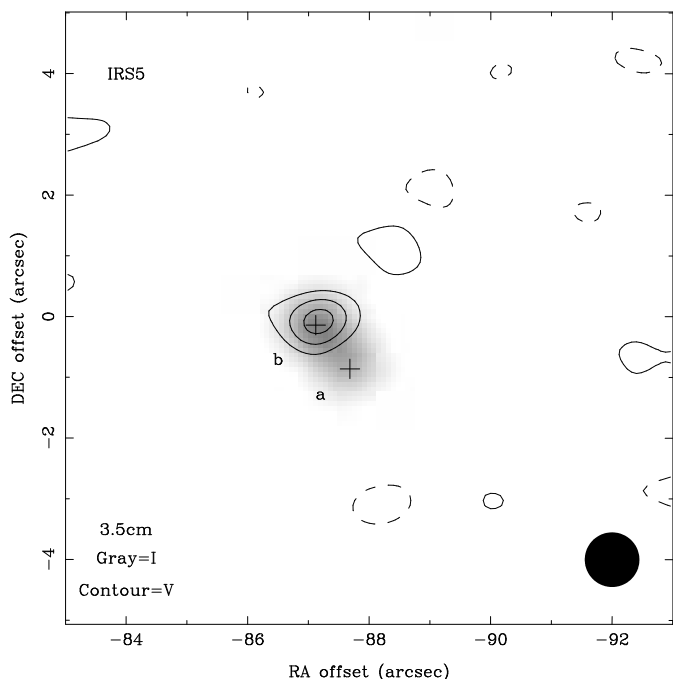


Fig. 2.— Stokes  $V$  map (contours) of the 3.5 cm continuum toward the IRS 5 region from high-resolution data sets: Tr 2, 4, and 13. A uniform-weight image was made from each data set. Each image was corrected for the primary beam response and convolved to an angular resolution of  $0.9''$  (shown in the bottom right corner), and then the three images were averaged. The contour levels are 1, 2, and 3 times  $0.04 \text{ mJy beam}^{-1}$ . Gray scale: Stokes  $I$  map as shown in Fig. 10 of Paper I. Plus signs: Peak positions of the 3.5 cm sources in the uniform-weight Stokes  $I$  map of Tr 1.

variations on 1998 July 19 (Tr 5). The source was unresolved, and the peak position was  $\alpha_{2000} = 19^{\text{h}}01^{\text{m}}55.31^{\text{s}}$ ,  $\delta_{2000} = -36^{\circ}57'21.7''$ , which agrees well (within  $0.4''$ ) with the position of IRS 7A determined from a higher-resolution map (see Table 2 of Paper I). The total flux was  $V = 0.19 \pm 0.02 \text{ mJy}$ . The fractional polarization cannot be exactly estimated because IRS 7A has both compact and extended components in the Stokes  $I$  map. Taking the intensity of the Stokes  $I$  map with uniform weighting as an upper limit on the  $I$  flux from the central compact source, the fractional polarization was  $\Pi_c \gtrsim 0.07$ .

Circularly polarized emission from B5 was detected during the observations on 2005 February 3 (Tr 13). The source was unresolved, and the peak position was  $\alpha_{2000} = 19^{\text{h}}01^{\text{m}}43.28^{\text{s}}$ ,  $\delta_{2000} = -36^{\circ}59'12.3''$ , which agrees well (within  $0.1''$ ) with the peak position of the Stokes  $I$  source from the same data set. The total flux was  $V = 0.26 \pm 0.04 \text{ mJy}$ , and the fractional polarization was  $\Pi_c = 0.12 \pm 0.02$ .

The other radio sources in the R CrA region were undetected in the  $V$  flux. These unpolarized sources are useful in checking the quality of the polarization calibration. If there had been a problem in the polarization calibration, strong sources would show a noticeable amount of apparent polarization systematically. IRS 7B, IRS 1, and IRS 2 are suitable for this purpose. Their  $|V|$  intensity was always less than  $0.05 \text{ mJy beam}^{-1}$ , and their  $\Pi_c$  was less than  $2\sigma$  level. Therefore, we conclude that the polarization calibration was good and that the detected  $V$  flux densities of IRS 5b, IRS 7A, and B5 do not include any significant contribution from instrumental effects.

## 4. DISCUSSION

### 4.1. IRS 5

IRS 5 is an interesting example of protobinary system. It is one of the youngest binaries with X-ray emission from both members, indicating that both have high-energy magnetic ac-

tivity (Hamaguchi et al. 2008). They displayed a concurrent enhancement of radio fluxes and were suggested to be interacting (Paper I). The projected separation of the binary is  $0.9''$ , which corresponds to 160 AU at a distance of 170 pc (Knude & Høg 1998). IRS 5 as a whole is a Class I source (Wilkning et al. 1997; Nutter et al. 2005; Paper I), but the accretion activity is weak. Nisini et al. (2005) derived an accretion rate of  $\sim 3 \times 10^{-8} M_{\odot} \text{ yr}^{-1}$  for IRS 5a (the rate for IRS 5b may be even smaller), which is much smaller than the accretion rate of other Class I objects such as IRS 1 and IRS 2 ( $2 \times 10^{-6} M_{\odot} \text{ yr}^{-1}$  and  $3 \times 10^{-7} M_{\odot} \text{ yr}^{-1}$ , respectively). IRS 5a/b may be Class I protostars with the accretion activity halted temporarily. (See White et al. 2007 for a discussion on the accretion rate of Class I protostars in general.) Nisini et al. (2005) suggested a spectral type of K5–K7V for IRS 5a, and the spectral type of IRS 5b is probably later than that.

#### 4.1.1. IRS 5b

While IRS 5b and 5a are comparable in the  $I$  flux, all the detectable  $V$  flux can be attributed to IRS 5b (Figs. 1 and 2), and separating them is important in the analysis of the source properties. Figure 3 shows the  $I$  and  $V$  light curves of IRS 5b, and Figure 4 shows the relation between  $I$  and  $V$ . The flux uncertainty shown in Figure 3 is the statistical uncertainty listed in Table 1, but one should also consider the uncertainty in the absolute flux scale, usually about 1%–2% (VLA Calibrator Manual).<sup>6</sup> However, the flux scale cancels out in the calculation of the ratio of flux densities, and only the statistical uncertainty needs to be considered for the fractional polarization.

The light curves of IRS 5b (Fig. 3) shows that  $V$  flux tends to be enhanced during the flare events. Such a trend is not obvious if IRS 5a/b are unresolved: Forbrich et al. (2006) thought

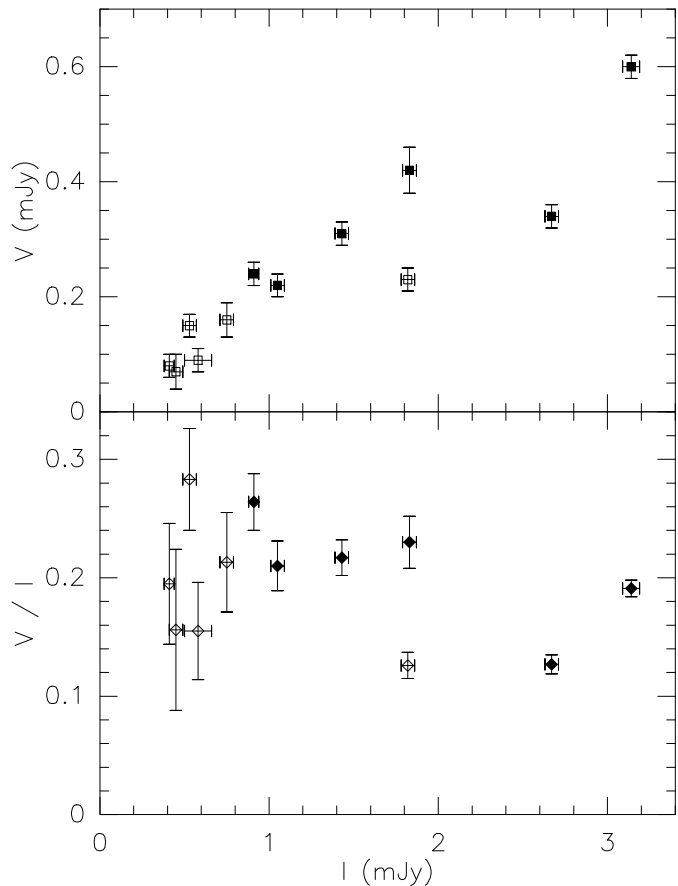


Fig. 4.— Stokes  $V$  flux (top panel) and fractional circular polarization (bottom panel) versus Stokes  $I$  flux density of IRS 5b at 3.5 cm. Filled markers: Data points of the active phase in 1998 September–October.

<sup>6</sup>See <http://www.vla.nrao.edu/astro/calib/manual>.

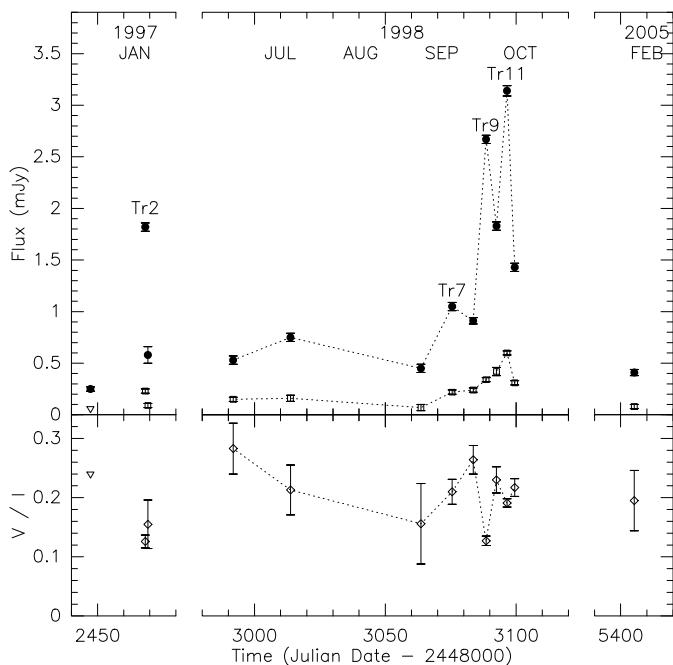


Fig. 3.— Light curves of IRS 5b at 3.5 cm. Filled circles: Stokes  $I$  flux densities. Open squares: Stokes  $V$  flux densities. Diamond symbols: Fractional circular polarization. Open triangles: Upper limits ( $3\sigma$ ) at Tr 1.

that the  $V$  flux appeared uncorrelated to the  $I$  flux because they were distracted by the flux variability of IRS 5a. Miettinen et al. (2008) also reported that the fractional polarization can be as high as 0.33, but their angular resolution was not high enough to make a clear interpretation. By separating IRS 5b from 5a, it is possible to make a detailed interpretation of the polarimetry results, as described below.

#### Helicity

The  $V$  flux was always positive (right-handed) during the 8 yr of monitoring. The helicity of emergent radiation is related to the configuration of magnetic fields (Morris et al. 1990). The constant helicity suggests that the magnetic field geometry responsible for the polarization is very stable and has a large scale (Mutel et al. 1987). Here, the large-scale geometry means a star-sized magnetosphere or an even larger structure. VLBI observations revealed that some RS CVn binaries have circumbinary halo and that some T Tauri stars have radio structures as large as 15 times the stellar radius (Mutel et al. 1985; Phillips et al. 1991). Dipole-like magnetospheric models are often employed to explain the radio observations of RS CVn binaries, T Tauri stars, and other radio stars (Güdel 2002). In the case of IRS 5b, the structure of the magnetosphere can be more complicated because it may possess a circumstellar disk.

As mentioned above, there is an overall correlation between the  $I$  and  $V$  light curves. During the active phase in 1998 (Tr 7–12), the signal-to-noise ratio is high enough that a more detailed description of the light curves is possible. While the  $I$  curve shows a relatively rapid fluctuation, the  $V$  curve varies slowly and shows only one peak (Fig. 3). The difference in the fluctuation timescale suggests that the  $I$  flux may respond to the energy injection relatively quickly and the  $V$  flux may come from a population of electrons having a longer relaxation timescale. This behavior can be explained by a core-halo model (Mutel et al. 1985; see the discussion below).

#### *I-V Correlation*

When only IRS 5b is considered, the correlation between  $I$  and  $V$  fluxes is quite good (Fig. 4). The  $V$  flux is roughly proportional to the  $I$  flux. The average value of  $\Pi_c$  is 0.17, and the standard deviation is 0.04. This good correlation strongly implies that the  $I$  and  $V$  fluxes come from the same source of energy and that the radiation mechanisms in the active phase and in the quiescent phase are basically the same.

If the quiescent radio emission is caused by frequent injections of energetic electrons through microflares (Güdel 2002), radio luminosity is expected to be related to X-ray luminosity. The 3.5 cm flux density of IRS 5b in the quiescent phase is  $\sim 0.5$  mJy (Paper I), and the radio luminosity is  $L_R \approx 1.7 \times 10^{16}$  erg s $^{-1}$  Hz $^{-1}$ . The X-ray luminosity of IRS 5b is  $L_X = 1.9 \times 10^{30}$  erg s $^{-1}$  (Hamaguchi et al. 2008). Then the ratio is  $L_X/L_R = 1.1 \times 10^{14}$  Hz, which is consistent with the empirical value of  $10^{15 \pm 1}$  Hz for active stars (Güdel 2002). (See also the  $L_R$ - $L_X$  relationship discussed by Feigelson et al. 1998 and Forbrich et al. 2006.) Therefore, the quiescent radio emission of IRS 5b is phenomenologically similar to what is observed in active late-type stars.

Figure 4 shows that the relation between  $\Pi_c$  and  $I$  is unclear when all data are considered. If the attention is restricted to the active phase only ( $I > 0.8$  mJy), the scatter of  $\Pi_c$  is smaller, and  $\Pi_c$  seems to be a weakly decreasing function of  $I$ . This trend is clearer if only the active phase of 1998 is considered. Such a behavior was also found in some radio active stars: the fractional circular polarization of RS CVn binaries and Algol decreases with increasing luminosity (Mutel et al. 1987, 1998). This anticorrelation was explained using a model in which the quiescent emission comes from an optically thin region (halo) of low Lorentz factor ( $\gamma \lesssim 5$ ) while the intense flare emission comes from an optically thick region (core) of more energetic electrons (Mutel et al. 1985, 1987).

#### *Strength of Magnetic Fields*

The emission mechanism of circularly polarized radio emission at centimeter wavelength is nonthermal gyrosynchrotron emission, and the detection of  $V$  flux at centimeter wavelength implies that the strength of the magnetic fields in the source region is a few hundred gauss or larger (Güdel 2002). The turnover frequency,  $\nu_{\text{peak}}$ , is a good indicator of the field strength. For example, White et al. (1989) derived a simple relation for a dipole source with typical parameters of M dwarf stars,

$$\nu_{\text{peak}} = 4.2(B_0/1000)^{0.76} \text{ GHz}, \quad (1)$$

where  $B_0$  is the surface magnetic field strength in G. In the quiescent phase, IRS 5b is brighter than IRS 5a, and the spectral

index of IRS 5b in the 4.9–8.5 GHz range is flat or slightly negative (Paper I). Then the turnover frequency of IRS 5b may be roughly in this frequency range, and the inferred field strength is  $B_0 \approx 2$  kG.

#### *4.1.2. IRS 5a*

While IRS 5a is more active in X-rays than IRS 5b, as it frequently showed solar type X-ray flares (Hamaguchi et al. 2008), it never showed polarized radio emission. The nondetection of circular polarization of IRS 5a is not simply owing to the relatively low  $I$  flux, because  $V$  flux was undetected even in the strong flare event of Tr 4. The  $3\sigma$  upper limit on the polarization fraction is 0.03. Therefore, while both radio polarization and X-ray emission are related to magnetic activity, there is no simple correlation between polarized radio flux and X-ray flares.

IRS 5a and 5b are quite similar in many aspects. They have comparable X-ray luminosities and almost identical X-ray spectra in the quiescent phase (Hamaguchi et al. 2008). Since they are in a binary system, they must have a similar age and are in the same environment. Then what causes the difference in the polarization of radio emission? A possible answer is the source geometry. It is well known that the fractional circular polarization of RS CVn binaries is dependent on the inclination angle of the system (Mutel et al. 1987, 1998; Morris et al. 1990). If this dependency is applicable to the IRS 5 system, it suggests that the magnetosphere of IRS 5b may have a pole-on configuration while that of IRS 5a may be equator-on.

#### *4.1.3. Peculiarity of IRS 5*

IRS 5b is the only known protostellar object persistently displaying circularly polarized radio emission. While this gives us a good opportunity to study the magnetic activity of protostars, it raises a question: why IRS 5b is an exception to the rule that the protostellar magnetosphere is hidden behind the free-free photosphere (the surface where the optical depth of free-free radiation equals unity)? That is, IRS 5b has either an unusually small free-free photosphere or an unusually large magnetosphere. Possible answers may include a small mass-loss rate (decreased ionized wind), a circumstellar disk with an inner hole (lack of disk-driven warm wind), and/or large-scale magnetic fields generated by disk dynamo (a disk-scale magnetosphere) (André et al. 1992, Tout & Pringle 1996).

Another unusual trait of IRS 5 is that it is the only known protostellar binary system with both members detected in X-rays (Hamaguchi et al. 2008). An interesting issue is the effect on the ionization of disk material because an accretion disk in such a system is illuminated by two X-ray sources. In terms of energy, only a small fraction of the X-ray photons from a star can illuminate the disk around its companion. (For example, a face-on disk with a radius about a third of binary separation would intercept less than 3% of the luminosity of the companion star.) However, this extra X-ray source can irradiate the disk from above if the binary system is not coplanar, and the ionizing photons can penetrate into the disk midplane relatively easily. In addition, such an effect can generate some asymmetry in the disk. Study of the dynamics and chemistry of accretion disks in such an environment would be useful because many stars form as members of multiple systems. A circumstellar disk in a multiple system may go through the X-ray irradiation not only from the host star but also from its companion at some point during the protostellar evolution.

#### 4.2. IRS 7A

The evolutionary status of IRS 7A is unclear (see § 5.1.1 of Paper I) because the spectral energy distribution (SED) is poorly constrained. IRS 7A is definitely not a Class II object (T Tauri star). The X-ray characteristics of IRS 7A is similar to that of Class I objects (Hamaguchi et al. 2005). The mid-IR SED of IRS 7A is similar to that of the Class 0/I transitional object IRS 7B (also see the color-color diagram in Paper I), but IRS 7A is less embedded than the nearby Class 0 source SMA 2 (Groppi et al. 2007). IRS 7A displays an outflow activity (Paper I), suggesting that accretion is also active. Considering all these facts, IRS 7A is most likely a protostar in the early part of the Class I stage. Then it is the youngest known object detected in circularly polarized radio emission, or a protostar showing an evidence of magnetosphere with an organized field configuration and a field strength of the order of 10–100 G.

Circularly polarized flux from IRS 7A was detected only once out of the 13 observing tracks reported here (Fig. 5). In addition, Suters et al. (1996) and Forbrich et al. (2007) also made Stokes  $V$  maps of the R CrA region but did not report any detection at the position of IRS 7A. Therefore, IRS 7A must be displaying a detectable circular polarization only rarely. However, at the epoch of the detection (Tr 5), the  $I$  flux was not particularly high. In fact, the  $I$  flux was on the low side of the scatter (see Table 4 of Forbrich et al. 2006). Even if we consider the intensity at the position of IRS 7A in uniform-weight maps (to minimize the blending of flux from the extended outflow),

the  $I$  intensity at Tr 5 is on the weaker side. This difference between  $I$  and  $V$  fluxes obviously shows that most of the  $I$  flux comes from a thermal source (Paper I) and only a fraction of  $I$  flux can be directly associated with the  $V$  flux. Therefore, if the angular resolution had been high enough to separate the thermal and nonthermal sources, the fractional circular polarization of the nonthermal emission must have been much higher than 0.07 (see § 3).

In contrast to the radio  $V$  flux, the X-ray emission of IRS 7A was detectable most of the time (Hamaguchi et al. 2005; Forbrich et al. 2006, 2007). Then an active magnetosphere probably exists all the time, and nonthermal radio emission may persist at some level. If so, why is the circular polarization usually undetectable? In fact, the nondetection is not surprising because the radio emission from the peristellar region of protostars is supposed to be obscured owing to the free-free absorption by the partially-ionized thermal winds (André et al. 1992). Then the question becomes how the radiation from the magnetosphere survived the absorption at the epoch of detection? Several possibilities can be suggested. First, the magnetosphere momentarily grew very large. Either the whole magnetosphere expanded or a portion of it stretched out. Second, the free-free photosphere shrank temporarily. This rarefaction of wind can happen if the mass-loss rate (hence the accretion rate) decreases for some reason. Third, the thermal wind was far from spherical and allowed an occasional direct view of the magnetosphere. Such a favorable line-of-sight can be achieved if the wind is collimated and changes directions. In principle, these possibilities can be tested using the VLBI technique although the transient nature of the phenomenon will be a major difficulty.

#### 4.3. Magnetic Fields of Protostars

If we take IRS 7A and IRS 5b as indicative examples of the evolution of magnetically active Class I objects, for lack of other examples, a plausible picture emerges: Most X-ray emitting Class I protostars may have magnetospheres. Younger ones, such as IRS 7A, may hide the existence of organized magnetic fields most of the time because the mass-loss rate is usually high and the wind is optically thick. Older protostars, such as IRS 5b, have a decreased level of mass loss, the wind becomes optically thin, and the magnetosphere becomes easily visible. (See the discussion by André et al. 1992.) The obvious next question is whether such magnetospheres exist around Class 0 protostars. Since there is no bona fide Class 0 object with detectable X-ray emission, the answer to this question may be hard to get. (This issue may be somewhat controversial because IRS 7B is around the verge of the Class 0 protostar category. See Hamaguchi et al. 2005 for more discussions on the implications of X-ray emission from IRS 7B.) A good starting point may be monitoring observations of X-ray-emitting young protostars such as IRS 7B. Another possible strategy is monitoring observations of Class 0 protostars that are weak in free-free emission. In this respect, the detection of circularly polarized 6 cm emission from the very low luminosity object L1014-IRS warrants further investigations of similar objects (Shirley et al. 2007).

The protostellar magnetosphere plays an important role in the circumstellar accretion and the accretion of matter in the inner disk. Theoretical models and observational characterization are relatively well developed for T Tauri stars, but not much is known about protostellar magnetospheres. Results of radio polarimetry, as reported in this paper, are beginning to provide valuable information on this important issue. The radio properties of IRS 7A and IRS 5b imply that the magnetic activity of Class I protostars are qualitatively similar to those of T Tauri

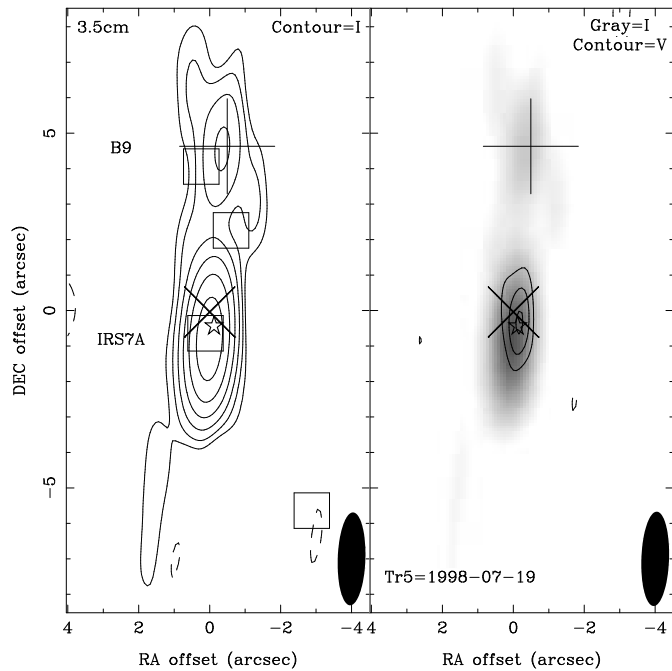


Fig. 5.— Natural-weight maps of the 3.5 cm continuum toward the IRS 7A region from track Tr 5. Shown in the bottom right corner is the synthesized beam: FWHM =  $2.6'' \times 0.8''$  and P.A. =  $-2^\circ$ . *Left panel*: Stokes  $I$  map. The contour levels are 1, 2, 4, 8, 16, and 32 times  $0.06 \text{ mJy beam}^{-1}$ . *Right panel*: Stokes  $V$  map (contours) superposed on the Stokes  $I$  map (gray scale). The contour levels are 1, 2, and 3 times  $0.06 \text{ mJy beam}^{-1}$ . *Plus sign*: The 1.1 mm continuum source SMA 2 (Groppi et al. 2007). *Cross*: X-ray source CXOU J190155.3-365722 (Hamaguchi et al. 2005). *Star symbol*: Mid-IR source IRAC 5 (Groppi et al. 2007). *Squares*: The 7 mm continuum sources (Choi & Tatematsu 2004).

stars. Future telescopes with better sensitivity and higher angular resolution should be able to help us understand the role of magnetic processes in protostellar evolution, and monitoring observations are crucial because of the time variability of these sources.

#### 4.4. Frequency Dependence of Polarization

All the three sources displaying circularly polarized emission at 3.5 cm did not show any detectable polarization at 6.2 cm. Such a frequency dependence is consistent with the observed properties of other magnetically active stars such as RS CVn systems: the fractional polarization tends to increase with frequency in the 5–15 GHz range (White & Franciosini 1995; García-Sánchez et al. 2003). However, it is not easy to explain this behavior using simple theoretical models of gyrosynchrotron radiation, and inhomogeneous models were suggested (Jones et al. 1994; White & Franciosini 1995). It is unclear how magnetically active protostars would behave over a wide range of frequency, and multifrequency observations of IRS 5b will be interesting.

#### 4.5. B5

B5 is a radio source with rapid flux variability (Brown 1987; Suters et al. 1996). It is not an extragalactic source, but its nature is poorly known (Paper I). Feigelson et al. (1998) suggested that B5 is a brown dwarf, but we cannot rule out the possibility that it may be a background object located much further away than the Cr A cloud.

Circularly polarized emission from B5 was never reported before and detected only once (Tr 13) out of the 13 observing tracks (Fig. 6). The  $I$  flux during Tr 13 was larger than the flux at the other epochs by a factor of  $\sim 3$  (see Fig. 2 of Pa-

per I). The fractional polarization during Tr 13 was also higher than the other epochs because polarized flux must have been detectable most of the time if  $\Pi_c$  were constant. This enhancement of  $I$  and  $\Pi_c$  during Tr 13 suggests that B5 seems to have gone through an outburst of highly polarized radio emission. Interestingly, the quiescent emission is also nonthermal because the spectral index during Tr 1 is highly negative (see Table 3 of Paper I). Then the radio emission structure of B5 must be peculiar: the quiescent emission may be synchrotron radiation from a large-scale structure, and the intense flare emission may be gyrosynchrotron radiation from a compact structure, probably a peristellar magnetosphere. Since the 6.2 cm source is extended and has a position offset with respect to the 3.5 cm source (Paper I), the large-scale structure is probably an outflow.

If B5 is a brown dwarf as suggested by Feigelson et al. (1998), it joins the small list of substellar objects detected in circularly polarized radio emission (Berger et al. 2001; Berger 2006). These objects show much higher radio luminosity than what is expected from the X-ray luminosity, which may explain the nondetection of B5 in X-rays. It is not well understood how such cool dwarfs can generate large-scale magnetic fields (Berger 2006).

On the other hand, the peculiar emission structure suggests a quite different possibility: B5 may be an exotic object containing a magnetically active compact source that is ejecting material at a highly relativistic speed. But it is certainly not an X-ray binary because no X-ray detection was ever reported. The nature of B5 is still an open question.

## 5. SUMMARY

The R CrA region was observed using the VLA in the 3.5 and 6.2 cm continuum to image the young stellar objects and study the star forming activity in this region. In addition, archival VLA data from recent observations made in extended configurations were analyzed. The results based on the imaging of Stokes  $I$  intensity were reported in Paper I, and the results of Stokes  $V$  imaging are reported in this paper. A total of 3 sources was detected in the 3.5 cm Stokes  $V$  flux while none was detected in the 6.2 cm circularly polarized continuum. The main results are summarized as follows:

1. Circularly polarized emission from IRS 5 was detected most of the time, and the exact source of the  $V$  flux was identified as IRS 5b. When IRS 5a and 5b are separated, there is a good correlation between the  $I$  and  $V$  fluxes of IRS 5b. The circular polarization is present at a  $\sim 17\%$  level, even in the quiescent phase, as long as the sensitivity is high enough to detect the  $V$  flux.

2. The  $V$  flux from IRS 5b was always positive over the 8 yr of monitoring, suggesting that the magnetosphere has a stable configuration. During the active (flaring) phases, when the signal-to-noise ratio is high enough, the fractional polarization is a weakly decreasing function of  $I$  flux. The active phases of IRS 5b last about a month or longer, and the light curve of  $V$  flux varies more slowly than that of  $I$  flux, which suggests that the source of the circularly polarized emission is huge in size. These properties suggests that IRS 5b is phenomenologically similar to other types of flare stars and has a very large magnetic structure.

3. IRS 5a was never detected in the circularly polarized radio continuum even during flares. The cause of the difference between IRS 5a and 5b is unclear, but a geometrical effect is possible.

4. Circularly polarized flux from IRS 7A was detected once

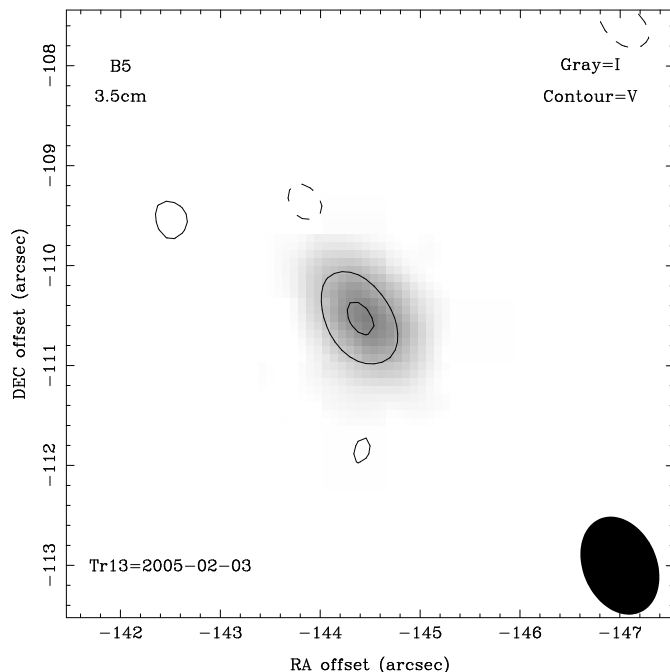


Fig. 6.— Stokes  $V$  natural-weight map (*contour*) of the 3.5 cm continuum toward the B5 region from track Tr 13. The contour levels are 1 and 2 times  $0.12 \text{ mJy beam}^{-1}$ . Shown in the bottom right corner is the synthesized beam: FWHM =  $1.0'' \times 0.7''$  and P.A. =  $23^\circ$ . *Gray scale*: Stokes  $I$  map as shown in Fig. 14 of Paper I.

out of the 13 observing tracks analyzed. The fractional circular polarization was at least 7%. Since IRS 7A drives a thermal radio jet, it is unclear how the polarized flux was not completely absorbed by the thermal wind.

5. Considering the properties of IRS 7A and IRS 5b, we suggest that most (X-ray emitting) Class I protostars may have magnetospheres and that the detection of radio emission from the magnetosphere becomes easier as the protostar evolves and the mass-loss rate decreases. Future surveys of similar Class I sources with the Expanded Very Large Array will be very exciting because the continuum sensitivity will be improved by an order of magnitude, and it may be possible to test the hypothesis above.

6. Circularly polarized emission from B5 was detected once, and the fractional circular polarization was 12%. B5 was in an outburst when the  $V$  flux was detected. While the detection of circular polarization shows that there is an organized magnetic field structure, the nature of B5 is still unclear.

We thank Y. L. Shirley and J. Cho for helpful discussions and suggestions. M. C. was supported by the Korea Science and Engineering Foundation (KOSEF) through the grant of the basic research program R01-2007-000-20196-0. K. H. is supported by the NASA Astrobiology Program under CAN 03-OSS-02. J.-E. L. gratefully acknowledges the support by KOSEF under a cooperative agreement with the Astrophysical Research Center for the Structure and Evolution of the Cosmos (ARCSEC). The National Radio Astronomy Observatory is a facility of the National Science Foundation operated under cooperative agreement by Associated Universities, Inc.

#### REFERENCES

- André, P. 1996, in ASP Conf. Ser. 93, *Radio Emission from the Stars and the Sun*, ed. A. R. Taylor & J. M. Paredes (San Francisco: ASP), 273
- André, P., Deeney, B. D., Phillips, R. B., & Lestrade, J.-F. 1992, *ApJ*, 401, 667
- Balbus, S. A., & Hawley, J. F. 1991, *ApJ*, 376, 214
- Berger, E. 2006, *ApJ*, 648, 629
- Berger, E., et al. 2001, *Nature*, 410, 338
- Bouvier, J., Alencar, S. H. P., Harries, T. J., Johns-Krull, C. M., & Romanova, M. M. 2007, in *Protostars and Planets V*, ed. B. Reipurth, D. Jewitt, & K. Keil (Tucson: Univ. Arizona Press), 479
- Brown, A. 1987, *ApJ*, 322, L31
- Camenzind, M. 1990, *Rev. Mod. Astron.*, 3, 234
- Choi, M., Hamaguchi, K., Lee, J.-E., & Tatematsu, K. 2008, *ApJ*, in press (Paper I)
- Choi, M., & Tatematsu, K. 2004, *ApJ*, 600, L55
- Feigelson, E. D., Carkner, L., & Wilking, B. A. 1998, *ApJ*, 494, L215
- Feigelson, E., Townsley, L., Güdel, M., & Stassun, K. 2007, in *Protostars and Planets V*, ed. B. Reipurth, D. Jewitt, & K. Keil (Tucson: Univ. Arizona Press), 313
- Forbrich, J., Preibisch, T., & Menten, K. M. 2006, *A&A*, 446, 155
- Forbrich, J. et al. 2007, *A&A*, 464, 1003
- García-Sánchez, J., Paredes, J. M., & Ribó, M. 2003, *A&A*, 403, 613
- Groppi, C. E., Hunter, T. R., Blundell, R., & Sandell, G. 2007, *ApJ*, 670, 489
- Güdel, M. 2002, *ARA&A*, 40, 217
- Hamaguchi, K., Choi, M., Corcoran, M. F., Choi, C.-S., Tatematsu, K., & Petre, R. 2008, *ApJ*, in press
- Hamaguchi, K., Corcoran, M. F., Petre, R., White, N. E., Stelzer, B., Nedachi, K., Kobayashi, N., & Tokunaga, A. T. 2005, *ApJ*, 623, 291
- Jones, K. L., Stewart, R. T., Nelson, G. J., & Duncan, A. R. 1994, *MNRAS*, 269, 1145
- Knude, J., & Høg, E. 1998, *A&A*, 338, 897
- Königl, A. 1991, *ApJ*, 370, L39
- Miettinen, O., Kontinen, S., Harju, J., & Higdon, J. L. 2008, *A&A*, 486, 799
- Morris, D. H., Mutel, R. L., & Su, B. 1990, *ApJ*, 362, 299
- Mutel, R. L., Lestrade, J. F., Preston, R. A., & Phillips, R. B. 1985, *ApJ*, 289, 262
- Mutel, R. L., Molnar, L. A., Waltman, E. B., & Ghigo, F. D. 1998, *ApJ*, 507, 371
- Mutel, R. L., Morris, D. H., Doiron, D. J., & Lestrade, J. F. 1987, *AJ*, 93, 1220
- Nisini, B., Antonucci, S., Giannini, T., & Lorenzetti, D. 2005, *A&A*, 429, 543
- Nutter, D. J., Ward-Thompson, D., & André, P. 2005, *MNRAS*, 357, 975
- Phillips, R. B., Lonsdale, C. J., & Feigelson, E. D. 1991, *ApJ*, 382, 261
- Preibisch, T., & Feigelson, E. D. 2005, *ApJS*, 160, 390
- Pudritz, R. E., Ouyed, R., Fendt, C., & Brandenburg, A. 2007, in *Protostars and Planets V*, ed. B. Reipurth, D. Jewitt, & K. Keil (Tucson: Univ. Arizona Press), 277
- Shirley, Y. L., Claussen, M. J., Bourke, T. L., Young, C. H., & Blake, G. A. 2007, *ApJ*, 667, 329
- Suters, M., Stewart, R. T., Brown, A., & Zealey, W. 1996, *AJ*, 111, 320
- Tout, C. A., & Pringle, J. E. 1996, *MNRAS*, 281, 219
- White, R. J., Greene, T. P., Doppmann, G. W., Covey, K. R., & Hillenbrand, L. A. 2007, in *Protostars and Planets V*, ed. B. Reipurth, D. Jewitt, & K. Keil (Tucson: Univ. Arizona Press), 117
- White, S. M., & Franciosini, E. 1995, *ApJ*, 444, 342
- White, S. M., Kundu, M. R., & Jackson, P. D. 1989, *A&A*, 225, 112
- Wilking, B. A., McCaughrean, M. J., Burton, M. G., Giblin, T., Rayner, J. T., & Zinnecker, H. 1997, *AJ*, 114, 2029